Noscapine induces apoptosis in human glioma cells by an apoptosis-inducing factor-dependent pathway

Elizabeth W. Newcomb[a,c], Yevgeniy Lukyanov[a,*], Iva Smirnova[a,*], Tona Schnee[a] and David Zagzag[a,b,c]

Previously, we identified noscapine as a small molecule inhibitor of the hypoxia-inducible factor-1 pathway in hypoxic human glioma cells and human umbilical vein endothelial cells. Noscapine is a nontoxic ingredient in cough medicine currently used in clinical trials for patients with non-Hodgkin's lymphoma or chronic lymphocytic leukemia to assess antitumor efficacy. Here, we have evaluated the sensitivity of four human glioma cell lines to noscapine-induced apoptosis. Noscapine was a potent inhibitor of proliferation and inducer of apoptosis. Induction of apoptosis was associated with activation of the c-jun N-terminal kinase signaling pathway concomitant with inactivation of the extracellular signal regulated kinase signaling pathway and phosphorylation of the antiapoptotic protein Bcl-2. Noscapine-induced apoptosis was associated with the release of mitochondrial proteins apoptosis-inducing factor (AIF) and/or cytochrome *c*. In some glioma cell lines, only AIF release occurred without cytochrome *c* release or poly (ADP-ribose) polymerase cleavage. Knock-down of AIF decreased noscapine-induced apoptosis. Our results suggest the potential importance of noscapine as a novel agent for use in patients with glioblastoma owing to its low toxicity profile and its potent anticancer activity. ***Anti-Cancer Drugs*** **19:553–563 © 2008 Wolters Kluwer Health | Lippincott Williams & Wilkins.**

Anti-Cancer Drugs 2008, **19**:553–563

Keywords: apoptosis, apoptosis-inducing factor-dependent pathway, Bcl-2 phosphorylation, noscapine, tubulin-binding agent

[a]Department of Pathology, [b]Division of Neuropathology and Department of Neurosurgery and [c]New York University Cancer Institute, New York University School of Medicine, New York, USA

Correspondence to Dr Elizabeth W. Newcomb, PhD, Department of Pathology, MSB128, New York University School of Medicine, 550 First Avenue, NY 10016, USA
Tel: +1 212 263 8757; fax: +1 212 263 8211;
e-mail: newcoe01@med.nyu.edu

*Yevgeniy Lukyanov and Iva Smirnova contributed equally to the work.

Received 15 January 2008 **Revised form accepted** 6 March 2008

Introduction

The unique mechanism of action of paclitaxel (taxol) to stabilize microtubules was discovered over 20 years ago [1]. Paclitaxel is the prototype of the taxane family of antitumor drugs and its mechanisms of action along with several other microtubule binding agents are becoming better understood [2–6]. However, owing to the high tubulin content of neuronal tissues, all tubulin-binding agents tested clinically to date share a common side effect of neurotoxicity. Thus, there have been major efforts to identify or develop novel tubulin-binding drugs with improved toxicity profiles, as these agents have proven to be important drugs in the treatment of a wide variety of cancer types [6].

Noscapine, a member of the benzylisoquinoline class of alkaloids, is a microtubule stabilizing agent with several promising anticancer properties [7–10]. It has been widely used as a cough suppressant in Europe and Asia for decades with no evidence of toxicity in humans [8,11,12]. More recently, noscapine was shown to reduce mortality rate in stroke victims, again without toxic side effects [9]. It has pleiotropic effects *in vitro* associated with its ability to induce growth arrest, to induce apoptosis, and to inhibit angiogenic activity [7,8,10,13,14]. Noscapine's antitumor activity has been demonstrated in several animal models of cancer, including breast cancer, glioma, melanoma, and lymphoma [8,15–19]. Importantly, in the glioma animal model, noscapine showed no evidence of neurotoxicity in the mice [17]. Most recently, noscapine was approved for use in phase I/II clinical trials for patients with non-Hodgkin's lymphoma or chronic lymphocytic leukemia [20].

Given the fact that novel therapies are urgently needed for glioblastoma, as part of our ongoing effort to identify potential therapeutics for this devastating disease [7,21–26], we have evaluated the sensitivity of four human glioma cell lines to noscapine-induced apoptosis.

Materials and methods

Cells and reagents

Glioma cell lines (U87MG, U118MG, LN229, and T98G) were obtained from the American Type Culture Collection (Manassas, Virginia, USA). We selected a panel of glioma cell lines based on their differences in p53 and PTEN status that reflect those known to occur in human gliomas [27]. The p53 status was wild type in U87MG and mutant for U118MG, LN229, and T98G, whereas the

0959-4973

PTEN status was wild type in LN229 and mutant in U87MG, U118MG, and T98G [27]. Cell lines were cultured in 5% CO_2 and 95% humidified atmosphere at 37°C in Dulbecco's modified Eagle's medium (Gibco BRL, Grand Island, New York, USA) supplemented with 10% fetal bovine serum (FBS) (Atlanta Biologicals, Norcross, California, USA), 1% penicillin and streptomycin, and 2 mmol/l glutamine (Gibco BRL). Cells were split every 3 days to ensure logarithmic growth. All drugs and saponin were purchased from Sigma-Aldrich (St Louis, Missouri, USA). Noscapine hydrochloride (100 mmol/l) and staurosporine (STS) (1 mmol/l) were dissolved in dimethylsulfoxide and stock solutions were stored at –80°C. MitoTracker Orange CMTMRos was obtained from Molecular Probes (Eugene, Oregon, USA).

Cytotoxicity studies

For the time course experiments, glioma cells (5×10^5) were plated in 10-cm Nunc dishes (Naperville, Illinois, USA) in 10 ml of medium for 24 h at 37°C before the addition of noscapine (20–150 μmol/l). Adherent and nonadherent cells (total cells) were harvested at the appropriate time interval and assessed for cell viability by trypan blue dye exclusion assay in triplicate. The IC_{50} values were the drug concentrations needed to inhibit glioma cell proliferation by 50% at 24 h of drug exposure.

Cell cycle analysis

For cell cycle analysis, total cells were harvested from each culture condition at the appropriate time interval, washed in ice-cold phosphate-buffered saline (PBS), resuspended in 400 μl of ice-cold PBS, and diluted by drop-wise addition of 1 ml of 100% ethanol. After fixation of >1 h at 4°C, cells were resuspended in RNase A/propidium iodide (PI) mixture containing 0.5 mg/ml RNase A and 50 μg/ml PI in PBS. DNA content was used to distinguish each cell cycle phase using flow cytometry. Flow cytometry was performed on a Becton Dickinson FACSCalibur (San Jose, California, USA).

Detection of mitotic cells by flow cytometry

Total cells were harvested and fixed in ethanol as described above. Following fixation overnight at 4°C, cells were washed twice with 1% FBS/PBST (PBS with 0.1% Tween-20), and incubated in anti-MPM-2 monoclonal antibody (1 μg/ml) or anti-phospho-histone H3 rabbit polyclonal antibody (5 μg/ml) (Upstate Biotechnology, Lake Placid, New York, USA) for 1 h at room temperature. Cells were washed twice in 1% FBS/PBST and incubated in fluorescein isothiocyanate (FITC)-conjugated donkey antimouse antibody (1 : 300; Jackson ImmunoResearch Laboratories, Inc., West Grove, Pennsylvania, USA) for 1 h at room temperature. Cells were washed twice in PBS and resuspended in 50 μg/ml PI containing 0.5 mg/ml RNase A in PBS. Cells were analyzed on a Becton Dickinson FACSCalibur for cell cycle distribution and mitotic index (percentage of MPM-2-positive or phospho-histone H3 (p-H3)-positive cells containing 4N DNA content). Dot plots and histograms of the MPM-2 or PI signal were obtained using the CellQuest software (BD Biosciences, San Jose, California, USA).

Western blot analysis

Total cells were harvested from each culture condition at the appropriate time interval, washed with ice-cold PBS, and lysed in a buffer containing Triton X-100 and Nonidet P-40 supplemented with protease inhibitors. Quantitation of protein was carried out with the BCA reagent (Pierce, Rockford, Illinois, USA). Equal amounts of protein (30 μg) in the presence of 5% β-mercaptoethanol (Sigma-Aldrich) were electrophoresed on 7.5% [β-actin, cyclin B1, MPM-2, poly (ADP-ribose) polymerase (PARP)] or 12% [apoptosis-inducing factor (AIF), Bcl-2, cytochrome *c*, phospho-Cdc2, extracellular signal regulated kinase (ERK), phospho-ERK, p-H3, phospho-c-Jun, c-Jun, survivin] sodium dodecyl sulfate polyacrylamide gel electrophoresis (SDS-PAGE) gels. Proteins were transferred to Immobilon-P membranes (Millipore, Bedford, Massachusetts, USA) by electroblotting at 30 V overnight at 4°C. Membranes were blocked for 1 h with 5% nonfat milk in PBST. Immunoblotting was performed at 4°C overnight with the following antibodies: mouse antiactin monoclonal antibody used at 1 : 20 000 (clone C4; Chemicon International, Inc., Temecula, California, USA); mouse anti-Bcl-2 monoclonal antibody used at 1 : 2000 (clone 124; Dako, North America, Inc., Carpenteria, California, USA); rabbit anti-Bax polyclonal antibody used at 1 : 1000 (Cell Signaling Technology, Danvers, Massachusetts, USA); mouse anti-PARP monoclonal antibody used at 1 : 500 (Ab-2, Oncogene, San Diego, California, USA); rabbit antisurvivin polyclonal antibody used at 1 : 1000 (Novus Biologicals Inc., Littleton, Colorado, USA); mouse anticyclin B1 monoclonal antibody used at 1 : 1000 (Santa Cruz Biotechnology, Santa Cruz, California, USA); mouse anti-MPM-2 monoclonal antibody used at 1 : 2000 (Upstate Biotechnology); and rabbit anti-phospho-histone H3 (Ser^{10}) polyclonal antibody used at 1 : 1000 (Upstate Biotechnology); mouse anticytochrome *c* monoclonal antibody used at 1 : 1000 (BD Biosciences, San Jose, California, USA); rabbit anti-AIF polyclonal antibody used at 1 : 500 (Santa Cruz Biotechnology); rabbit anti-ERK1/2 polyclonal antibody used at 1 : 1000 (Cell Signaling Technology); mouse anti-phospho-ERK1/2 (Tyr^{204}) monoclonal antibody used at 1 : 500 (clone E-4; Santa Cruz Biotechnology); rabbit anti-phospho-Cdc2 (Tyr^{15}) polyclonal antibody used at 1 : 1000 (Cell Signaling Technology); rabbit anti-phospho-c-Jun (Ser^{63}) polyclonal antibody used at 1 : 1000; and rabbit anti-c-Jun monoclonal antibody used at 1 : 500 (Cell Signaling Technology). Sheep antimouse IgG and donkey antirabbit IgG (both from GE Healthcare, Buckingamshire, UK) horseradish peroxidase-conjugated secondary antibodies were used at 1 : 2000.

Immunodetection was carried out with the Supersignal West Femto or West Pico (for β-actin) Maximum Sensitivity Substrate detection system (Pierce) followed by densitometry using NIH Image software.

Cellular fractionation

Total cells were harvested, counted, and washed with PBS. Cells (1×10^6) were pelleted for 5 min at 800*g* and the cell pellet was lysed in 50 µl lysis buffer (80 mmol/l KCl, 250 mmol/l sucrose, 500 µg/ml digitonin, and protease inhibitors) and incubated for 10 min on ice. Cell lysates were centrifuged for 10 min at 10 000*g* at room temperature and samples were stored at −20°C. Proteins from the supernatant (cytosolic fraction) were analyzed by western blotting for cytochrome *c* and AIF.

Immunofluorescence microscopy for apoptosis-inducing factor, and cytochome *c*

Cells (3×10^4) were plated on poly-D-lysine-coated (0.1 mg/ml; Sigma-Aldrich) coverslips in 6-well plates and allowed to attach at 37°C for 24 h before the addition of the drug. To analyze the release of mitochondrial proteins (AIF, cytochrome *c*), the cells were untreated or treated with noscapine (100 µmol/l), fixed in 4% paraformaldehyde, permeabilized for 1 min in PBS/0.1% Triton X-100, and nonspecific binding sites were blocked with 2% FBS for 5 min. Cells were incubated with rabbit anti-AIF polyclonal antibody (1 : 100; Santa Cruz Biotechnology) or mouse anticytochrome *c* monoclonal antibody diluted 1 : 100 (BD Pharmingen, Inc., San Diego, California, USA) overnight at 4°C. The secondary FITC-conjugated antibodies were used in accordance with the manufacturer's instructions. Cells were washed twice with PBS and counterstained with PI (20 µg/ml) for 15 min at room temperature. Cells were washed three times with PBS and mounted onto Colorfrost Plus slides (Fisher Scientific, Pittsburgh, Pennsylvania, USA) using VectaShield Hardset (Vector Laboratories, Burlingame, California, USA). Images were captured on a Nikon Eclipse inverted fluorescence microscope with Spot digital camera and processed using Adobe Photoshop 9.0 software.

Detection of apoptosis-inducing factor by flow cytometry

Total cells were incubated for 30 min in media containing 0.1 µmol/l MitoTracker Orange CMTMRos (Molecular Probes, Eugene, Oregon, USA) at 37°C and then untreated or treated with noscapine (100 µmol/l). At the appropriate time interval, cells were harvested, fixed in 0.25% paraformaldehyde, and permeabilized for 5 min in PBS/0.01% saponin. Cells were incubated with primary rabbit anti-AIF polyclonal antibody (1 : 100; Santa Cruz Biotechnology) and diluted in PBS/0.01% saponin for 30 min at 4°C. Cells were washed and incubated with secondary FITC-conjugated goat antirabbit antibody (1 : 200; Jackson ImmunoResearch Laboratories, Inc.) for 30 min at 4°C. Nuclei were stained with Hoechst 33 342 (20 µg/ml; Sigma-Aldrich) for 3 min. The translocation of AIF from the mitochondria to nuclei was analyzed by flow cytometry (LSRII; Becton Dickinson) as described [28].

Transfection of U87MG glioma cells with small interfering RNA targeting apoptosis-inducing factor expression

U87MG cells were plated (3×10^5) in 60-mm dishes and after 24 h were transfected. Before transfection the medium was aspirated and 4.6 ml of serum-free medium was added to each plate. Knock-down of AIF expression was performed using validated target sequences (SI02662653; Qiagen, Valencia, California, USA). For transfection, 5 nmol annealed small interfering RNA (siRNA) targeting AIF or the AllStars negative control siRNA [a scrambled (Scr) sequence with no significant homology to any known gene sequences from mouse, rat, or human cell lines] was used. The siRNA sequences were diluted in serum-free medium, mixed with 4 µl Hiperfect (Qiagen), and incubated at room temperature for 10 min. The mixtures were added dropwise to each dish, mixed by gently swirling the dish, and incubated for 4 h at 37°C when 0.5 ml of FBS was added for a final concentration of 10%. After incubation at 37°C for 48 h, cultures were untreated or treated with noscapine (100 µmol/l) for 16 h. Cells were harvested for trypan blue exclusion assay and western blotting. Two independent experiments were performed. In a separate experiment, cells (1×10^5) were plated onto poly-D-lysine-coated coverslips in 6-well plates, transfected with the appropriate siRNAs, and processed for AIF immunofluorescence microscopy as described above.

Results

Noscapine inhibits cell proliferation

Treatment of U87MG, U118MG, LN229, and T98G glioma cell lines for 72 h with noscapine (20–150 µmol/l) resulted in a dose-dependent inhibition of cell proliferation. Data from three independent studies are summarized in Fig. 1. When glioma cell lines were treated with noscapine, cell proliferation was inhibited within 24 h of drug exposure. The IC_{50} values were 131 µmol/l for U87MG, 91 µmol/l for U118MG, 86 µmol/l for LN229, and 97 µmol/l for T98G. Given the response of the different cell lines to noscapine treatment, we chose the concentration of 100 µmol/l for all further experiments.

Noscapine induces M-phase arrest

Flow cytometry was used to determine DNA content and cell cycle phase (Fig. 2a), and expression of the mitosis-specific marker MPM-2 (Fig. 2b). Expression of both MPM-2 and p-H3 was analyzed by western blot analysis. Representative data for each of the four cell lines treated with noscapine for 24 h is shown from one of three independent experiments. All the cell lines demonstrated

Fig. 1

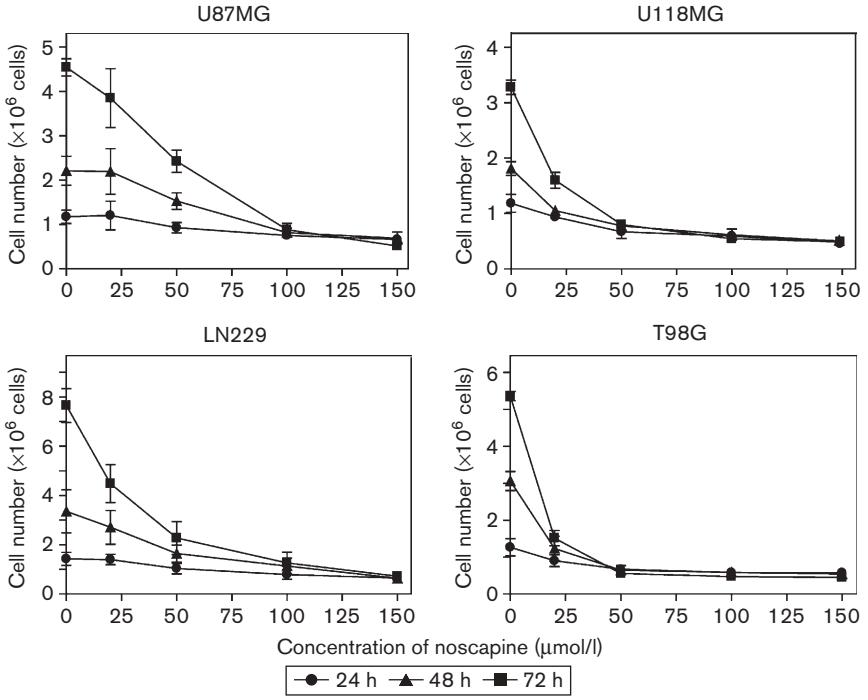

Noscapine inhibits cell proliferation. Cells were untreated or treated with noscapine at the indicated concentrations and times. At the appropriate time interval, total cells were harvested, counted to determine viability and cell number, and the total number of viable cells were plotted for each cell line. The results of three independent experiments are shown. Error bars indicate the range of the determinations (mean ± SD).

growth arrest at G_2/M within 24 h of noscapine treatment. Maximal cell death occurred within 48 h of drug exposure (data not shown).

As conventional flow cytometry does not distinguish between cells in G_2-phase of the cell cycle from those that are in M-phase, we analyzed the expression of the mitosis-specific markers MPM-2 and p-H3 [29,30] by flow cytometry (Fig. 2b) and by western blot analysis (Fig. 2c). Representative two-dimensional scatter plots of cells double positive for MPM-2 and 4N DNA content (PI staining) showed that the percentage of MPM-2 positive cells increased from a low background level of 2–4% in untreated cultures to 15–60% with noscapine treatment. Similar results were obtained when cells were immunostained with p-H3 and analyzed by flow cytometry (data not shown). Western blot analysis confirmed increased expression of both the MPM-2 and p-H3 mitosis-specific proteins at 24 h in noscapine-treated glioma cells compared with untreated cultures indicating M-phase arrest.

Noscapine alters expression of apoptosis and cell cycle-related proteins

As noscapine treatment induced M-phase arrest, we assessed changes in the expression patterns of several proteins involved in regulating apoptosis and the cell cycle, such as Bcl-2, Bax, cyclin B1, Cdc2, and survivin. Representative data from one of three independent experiments is shown in Fig. 3. Phosphorylation of Bcl-2 is induced by microtubule binding agents, including one recent report using noscapine [2,3,14,31,32]. Noscapine treatment of the glioma cell lines for 24 h induced phosphorylation of Bcl-2. The appearance of slower migrating forms of Bcl-2 on western blotting is consistent with its phosphorylation. The U118MG and LN229 cell lines showed two slower migrating bands, compared with only one in U87MG and T98G cell lines (Fig. 3). The presence of multiple phosphorylated forms of Bcl-2 have been noted previously by others in cells treated with microtubule binding agents [33,34]. In contrast, the levels of Bax remained unaltered.

Next, we evaluated the expression levels of the cell cycle proteins cyclin B1, Cdc2, and survivin. Representative data for changes in these proteins in glioma cell lines following 24 h of noscapine treatment are shown (Fig. 3). Cyclin B1 forms a complex with the Cdc2 kinase to regulate the entry of cells into G_2/M phase. Activation of Cdc2 kinase is associated with an increased expression of cyclin B1 resulting in cell cycle arrest at G_2/M phase [35]. Consistent with noscapine-induced M-phase arrest, the

Fig. 2

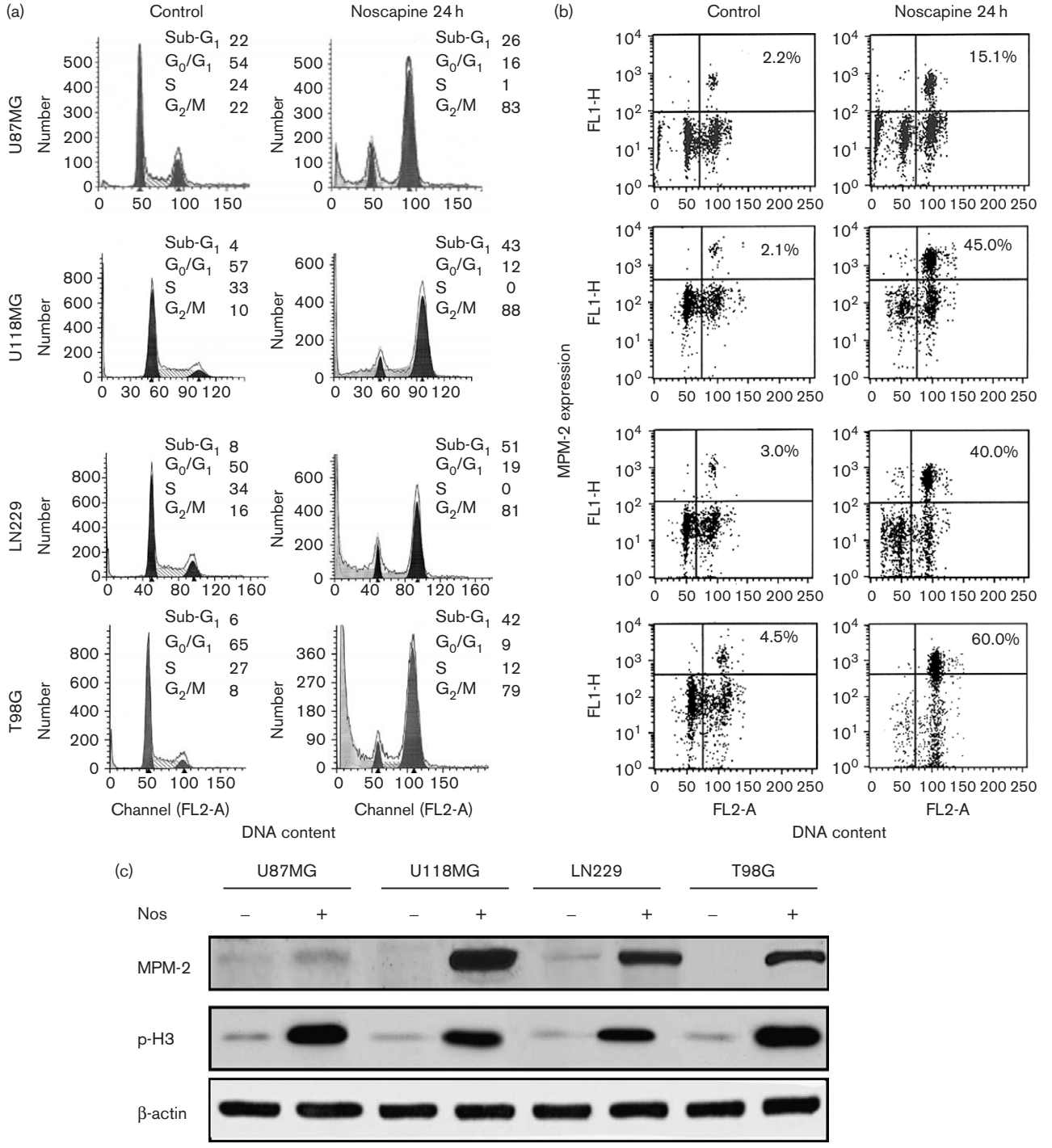

Noscapine induces M-phase arrest. Cells were untreated or treated with noscapine (100 μmol/l) for 24 h. (a) Total cells were harvested, stained with propidium iodide, and analyzed for cell cycle profiles by flow cytometry. The data presented are representative of three independent experiments. (b) Glioma cells were untreated or treated with noscapine (100 μmol/l) for 24 h, harvested, stained with anti-MPM-2 and propidium iodide, and analyzed by flow cytometry. Cells in the upper right quadrant are dual positive for MPM-2 and 4N DNA content. The results show two-dimensional dot plots from one of three independent experiments. (c) Glioma cells were untreated or treated with noscapine (100 μmol/l) for 24 h, harvested, and lysates subjected to western blotting with anti-MPM-2 and anti-phospho-histone H3 (p-H3) antibodies. β-Actin was used as the loading control. The results of one representative western blot are shown from one of two independent experiments. Nos, noscapine.

Fig. 3

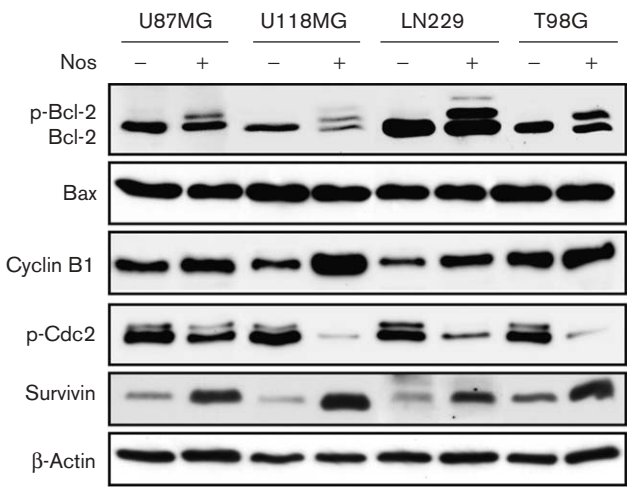

Noscapine alters expression of apoptosis and cell cycle-related proteins. Cells were untreated or treated with noscapine (100 μmol/l) for 24 h, harvested, and lysates subjected to western blotting with the appropriate antibodies. β-Actin was used as the loading control. The results of one representative western blot are shown from one of three independent experiments. Nos, noscapine.

Fig. 4

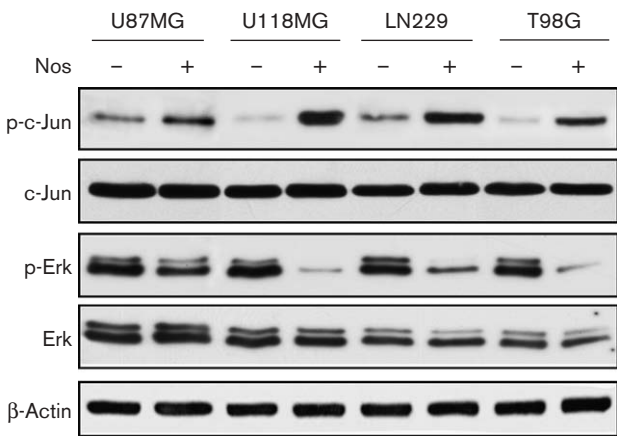

Noscapine differentially affects JNK and ERK MAPK signaling pathways. Cells were untreated or treated with noscapine (100 μmol/l) for 24 h, harvested, and lysates subjected to western blotting with the appropriate antibodies. β-Actin was used as the loading control. The results of one representative western blot are shown from one of two independent experiments. ERK MAPK, extracellular signal regulated kinase mitogen-activated protein kinases; JNK, c-jun N-terminal kinase. Nos, noscapine.

level of expression of cyclin B1 was increased. Activation of the mitotic spindle assembly checkpoint is associated with increased levels of phosphorylated histone H3 and reduced phosphorylation of Cdc2 on Tyr^{15}, an inhibitory phosphorylation site. Noscapine-treated cells showed a marked decrease in phospho-Cdc2 compared with untreated cells (Fig. 3) which is consistent with the upregulation of phospho-H3 (Fig. 2c) and increased Cdc2 kinase activity.

Survivin, a member of the chromosomal passenger complex that regulates cell division, is expressed in the G_2/M phase of the cell cycle and localizes to several sites on the mitotic apparatus, including centrosomes and microtubules in cells in M-phase [36]. When glioma cells were treated with noscapine, survivin levels increased greatly (Fig. 3). These results, taken together, indicate that changes in expression levels of cell cycle proteins that play important roles in regulating mitosis and the mitotic checkpoint are correlated with noscapine's ability to arrest cells in M-phase.

Noscapine differentially affects c-jun N-terminal kinase and extracellular signal regulated kinase mitogen-activated protein kinase signaling pathways

A characteristic response of cells treated with microtubule binding agents is activation of mitogen-activated protein kinases (MAPK), ERK, and c-jun N-terminal kinase (JNK) concomitant with induction of apoptosis [2–4,37–39]. We evaluated the phosphorylation status of c-Jun, a marker of JNK MAPK pathway activation, and phospho-ERK1/2, a marker of Ras-Raf MAPK pathway activation. Representative data for changes in the phosphorylated forms of these proteins in glioma cell lines following 24 h of noscapine treatment are shown from one of three independent experiments in Fig. 4. Activation of JNK causes phosphorylation of Ser^{63} on c-Jun and increased levels of phospho-c-Jun are clearly observed in noscapine-treated cells compared with untreated controls. These results are consistent with the upregulation of phospho-c-Jun reported for noscapine-treated human ovarian cancer cell lines [37].

In contrast to noscapine-induced activation of the JNK signaling pathway, the ERK MAPK signaling pathway was inactivated. Both phospho-ERK1/2 bands in noscapine-treated cells were markedly decreased compared with untreated cultures. Although activation of JNK is commonly observed in cells treated with microtubule binding agents, regardless of the interfering mechanism (stabilization vs. destabilization of microtubules), the reported effects of microtubule binding agents on ERK1/2 activity have varied from no effect, to inactivation, or activation [40–42]. The results reported here suggest that apoptosis induced by noscapine in glioma cells is correlated with activation of the JNK signaling pathway together with the inactivation of the ERK signaling pathway.

Noscapine induces apoptosis associated with release of mitochondrial proteins cytochrome *c* and apoptosis-inducing factor

To further explore the mechanism of noscapine-induced apoptosis, we determined whether mitochondrial injury occurred with the release of the mitochondrial proteins cytochrome *c* and/or AIF release. The results of representative western blots for PARP cleavage (Fig. 5a), cytochrome *c*, and AIF release (Fig. 5b) are shown from one of four independent experiments. The LN229 and T98G cell lines demonstrated the signature cleavage products for PARP (85 kDa) after 24 h of noscapine treatment that were undetectable in the U87MG and U118MG drug-treated cultures. Prolonged exposure to noscapine for up to 72 h in both U87MG and U118MG cell lines did not induce PARP cleavage (data not shown). In contrast, when the same four cell lines were treated for 24 h with staurosporine (1 μmol/l), a broad spectrum kinase inhibitor known to induce apoptosis, PARP cleavage was readily demonstrated (Fig. 5a). Cellular fractionation studies confirmed release of cytochrome *c* in only those cell lines that demonstrated PARP cleavage, whereas all cell lines showed increased levels of AIF released into the cytosol following noscapine treatment (Fig. 5b). Pretreatment of U87MG and U118MG glioma cell lines with the broad spectrum pan caspase inhibitor zVAD-fmk before noscapine treatment failed to block cell death (data not shown). This result is consistent with AIF-dependent apoptosis in the glioma cell lines.

Fig. 5

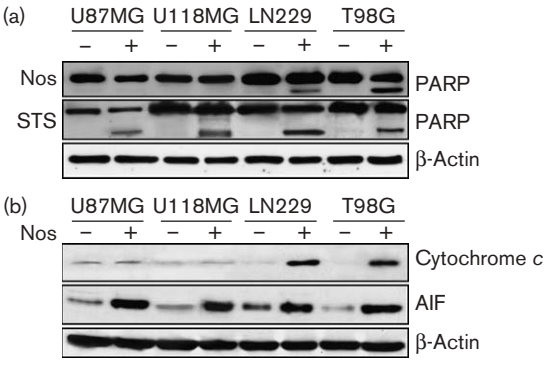

Noscapine induces apoptosis associated with release of mitochondrial proteins cytochrome *c* and AIF. (a) Cells were untreated or treated with noscapine (100 μmol/l) or staurosporine (1 μmol/l) for 24 h, harvested, and lysates subjected to western blotting with anti-PARP. The proform of PARP at 116 kDa and the cleavage product of 85 kDa are noted. β-actin was used as the loading control. The results of one representative western blot are shown from one of four independent experiments. (b) Cells were untreated or treated with noscapine (100 μmol/l) for 24 h, harvested, processed for cytosolic (supernatant) fractions, and lysates subjected to western blotting with anticytochrome *c* and anti-AIF antibodies. β-Actin was used as the loading control. The results of one representative western blot are shown from one of two independent experiments. AIF, apoptosis-inducing factor; Nos, noscapine; PARP, poly (ADP-ribose) polymerase; STS, staurosporine.

To confirm release of cytochrome *c* or AIF from the mitochondria, we performed immunofluorescence microscopy and flow cytometry on all cell lines. The representative results are shown for T98G and U87MG cell lines (Fig. 6). By immunohistochemistry, no release of cytochrome *c* was detectable in U87MG cells, where the mitochondria retained a punctate staining pattern (Fig. 6d) compared with T98G cells that showed a diffuse staining pattern in the cytosol (Fig. 6c). In contrast, noscapine treatment induced release of AIF from the mitochondria and translocation to the nucleus in both T98G and U87MG cells (Fig. 6g and h). Flow cytometry showed approximately a two-fold increase in AIF translocation to the nucleus in both cell lines (Fig. 6i and j).

Noscapine induces apoptosis-inducing factor-dependent cell death

To determine whether AIF played a role in noscapine-induced cell death, we performed knock-down of AIF expression in U87MG cells. The results of a representative western blot for AIF expression from one of two independent experiments (Fig. 7a) and cell viability (Fig. 7b) are shown. The experiment was repeated and the cells were processed for AIF immunofluorescence microscopy (Fig. 7c). AIF expression was decreased in cells transfected with siRNA directed to AIF compared with cells transfected with Scr siRNA. The knock-down of AIF was correlated with decreased cell death in noscapine-treated cultures (2.3 ± 0.2) compared with cultures treated with Scr siRNA and noscapine (6.2 ± 0.9). By immunofluorescence microscopy, knock-down of AIF in cells decreased the punctate staining of AIF in the mitochondria and prevented its translocation to the nucleus with noscapine treatment. In contrast, cells transfected with Scr siRNA showed translocation of AIF to the nucleus when treated with noscapine.

Discussion

Here we have evaluated the sensitivity of four human glioma cell lines to noscapine-induced apoptosis. We found that the IC_{50} values for the glioma cell lines ranged from 85 to 131 μmol/l, which differs from those reported for human lymphoid, melanoma, breast, and colon cell lines, most likely owing to differences in the cell types studied and their genetic alterations [14,16,19,37,43]. Similar to other microtubule binding agents, noscapine arrests cells in M-phase and alters the expression levels of cell cycle regulated proteins, such as increased expression of cyclin B1 and survivin and decreased levels of phospho-Cdc2, changes consistent with cells undergoing cell death by mitotic catastrophe [44,45].

Noscapine has been extensively analyzed for its mechanisms of action on microtubule dynamics and tubulin binding [8,10,13,16,18,19,37]. It appears to be unique

Fig. 6

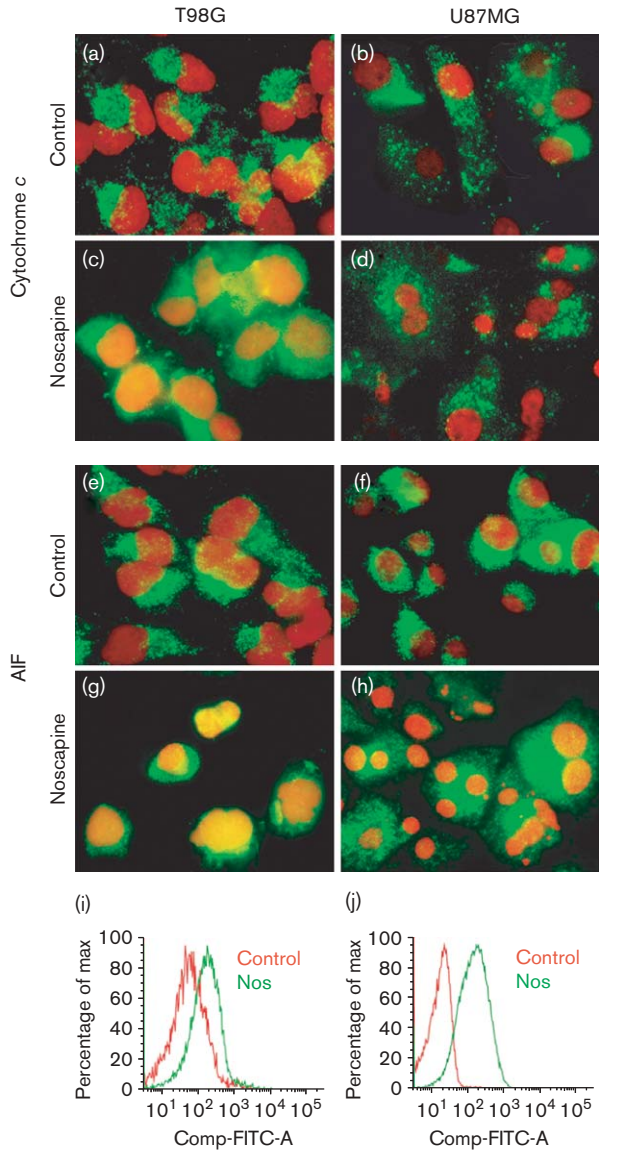

Noscapine induces release of cytochrome *c* to the cytosol and AIF translocation to the nucleus. The T98G (left column) and U87MG (right column) cell lines were untreated (a, b; e, f) or treated (c, d; g, h) with noscapine (100 µmol/l) for 16 h before immunohistochemistry for cytochrome *c* and AIF. Cells were fixed, permeabilized, and immunostained with anti-cytochrome *c* or anti-AIF antibody (green fluorescence) with counterstaining with PI (red fluorescence) to visualize nuclei. In T98G cells that undergo caspase-dependent apoptosis, noscapine-treated cells showed an increase in diffuse staining of cytochrome *c* in the cytoplasm (c) whereas in U87MG cells that undergo caspase-independent apoptosis, the cytocrome *c* staining in the cytoplasm remained punctate and associated with mitochondria (d). In contrast, in noscapine-treated T98G (g) and U87MG (h) cells, AIF translocated to the nucleus compared with untreated cells that retained the punctate cytosolic staining pattern of mitochondria (e, f). Yellow/orange nuclear pattern indicates colocalization of the AIF and PI staining. By flow cytometry, AIF release from mitochondria and translocation to the nucleus is shown for T98G (i) and U87MG (j) cell lines. Cells were stained and fluorescence quantified on a LSRII flow cytometer. Representative histograms of the fluorescence intensity of the nuclear fractions from untreated (red line) and noscapine-treated (green line) cells are shown from one of two independent experiments. Noscapine treatment induced a two-fold increase in nuclear AIF fluorescence accumulation. AIF, apoptosis-inducing factor; FITC, fluorescein isothiocyanate; Nos, noscapine; PI, propidium iodide.

among microtubule binding agents in that noscapine has subtle effects on microtubule steady-state dynamics. It neither promotes nor inhibits microtubule polymerization at concentrations of 100 µmol/l, but rather the microtubules spend an increased amount of time in a paused state, and as a result the total mass of tubulin remains unaltered [10]. This feature may explain its excellent toxicity profile demonstrated in both human and animal studies [8,9,15,19,20,46]. The differential effects of microtubule binding agents on tumor cells, in general, have been attributed to the fact that tumor cells are deficient in the mitotic spindle assembly checkpoint, whereas normal cells are proficient [2,4,6]. Taken together, these findings underscore the potential importance of noscapine as an anticancer agent for use in a wide variety of cancers owing to its preferential toxicity for tumor cells compared with normal cells.

In contrast to activation of the JNK pathway by noscapine in glioma cells, we observed inactivation of the ERK signaling pathway associated with decreased levels of expression of phospho-ERK but no activation of p38 (data not shown). Inactivation of ERK signaling has been reported for KB-3 human epidermoid cells treated with vinblastine, vincristine, taxol, or colchicines [41]. However, treatment of MCF-7 breast cancer cells with some of the same drugs, including vincristine, taxol, or colchicine, did not change the activity of ERK [40]. Signaling events controlling apoptosis are complex and require a balance between growth promoting (ERK) and stress inducing (JNK) signals [47]. Our data would imply that induction of apoptosis in certain cell types, such as glioma and epidermal carcinoma, is associated with activation of JNK concomitant with inactivation of ERK signaling pathways. Of note, recent studies have correlated the induction of apoptosis with the inactivation of ERK and AIF translocation from the mitochondria [48,49].

Apoptosis induced by two noscapine analogs in CEM lymphoblastoid cell lines and drug-resistant sublines of ovarian carcinoma cell lines was associated with activation of caspase-3 and subsequent PARP cleavage [13,18]. Most recently, noscapine-induced apoptosis in HL60 and K562 myeloid cells was associated with activation of several caspases and PARP cleavage [14]. In this study, we asked whether noscapine-induced cell death of glioma cells also occurred via a similar caspase-dependent pathway. The LN229 and T98G cell lines demonstrated the signature cleavage products of PARP within 24 h of noscapine treatment, whereas the U87MG and U118MG cell lines did not. When staurosporine was used in the same panel of cell lines, PARP cleavage was induced in all four glioma cell lines, indicating a caspase-dependent cell death. By western blotting and immunohistochemistry, we further confirmed that the presence of PARP cleavage was correlated with the cytochrome *c* release. In contrast, noscapine induced release of mitochondrial AIF in all cell

Fig. 7

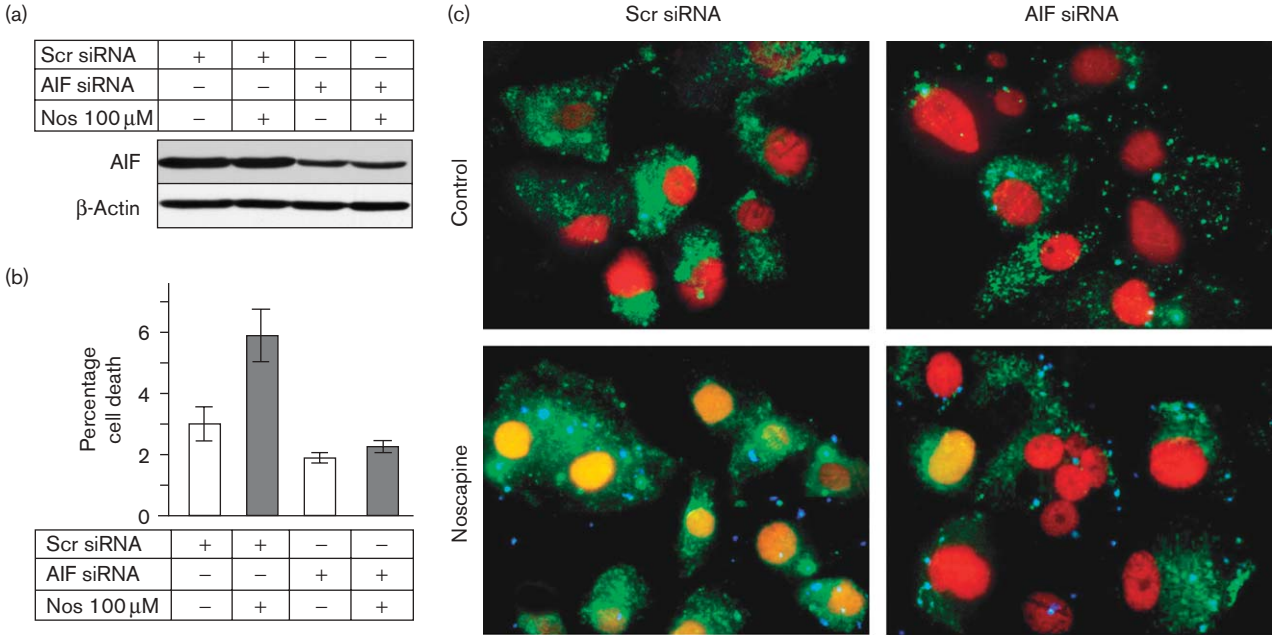

Noscapine induces AIF-dependent cell death. U87MG cells were transfected with scrambled (Scr) siRNA or siRNA directed to AIF. After 48 h, cells were treated with noscapine (100 μmol/l) for 16 h, and harvested for (a) western blotting with anti-AIF antibody and (b) trypan blue exclusion assay done in triplicate. The results of a representative experiment are shown from one of two independent experiments. (c) In a separate experiment, transfected U87MG cells were treated with noscapine (100 μmol/l) for 16 h before immunohistochemistry for AIF as described in the legend of Fig. 6. Cells were immunostained with anti-AIF antibody (green fluorescence) and counterstained with propidium iodide (red fluorescence) to visualize nuclear morphology. The siRNA molecules are tagged with Alexa 488 and appear as bright blue dots in transfected cells. Noscapine induced AIF translocation to the nucleus in cells transfected with Scr siRNA compared with rare cells with nuclear AIF localization in cells transfected with siRNA directed to AIF. AIF, apoptosis-inducing factor; Nos, noscapine; siRNA, small interfering RNA.

lines. To determine whether AIF played a role in cell death induced by noscapine treatment, we transfected U87MG cells with siRNA directed against AIF. Cell death in U87MG cells with knock-down of AIF expression was decreased compared with cells transfected with the Scr siRNA sequence. We have previously documented AIF release and caspase-independent apoptosis in flavopiridol-treated glioma cells [21], whereas mitotic catastrophe induced in glioma cells treated with geldanamycin was associated with the release of both cytochrome *c* and AIF [23]. Others have reported caspase-dependent as well as caspase-independent cell death in breast cancer cells treated with doxorubicin [50], caspase-dependent cell death in glioma cells treated with the novel cytokine melanoma differentiation associated gene-7/interleukin-24 [51], or caspase-independent but AIF-dependent cell death in glioma cells treated with a phosphoinositide-dependent kinase inhibitor OSU-03012 [52], similar to what we have observed here.

To our knowledge, there has only been one previous report showing induction of Bcl-2 phosphorylation by noscapine [14,43], despite the fact that Bcl-2 phosphorylation is considered one of the hallmark responses to microtubule binding agents [2,3]. Cells treated with microtubule binding agents induce the stress response kinase JNK that is responsible for the phosphorylation of Bcl-2 [2–4,53,54]. Normally, Bcl-2 functions as an inhibitor of apoptosis. However, its antiapoptotic activity can be inactivated by phosphorylation of specific residues in an unstructured loop of Bcl-2 [53]. Deletion of this loop region of Bcl-2 completely prevents apoptosis induced by the microtubule binding agent paclitaxel. The apoptosis signal-regulating kinase-1 phosphorylates Bcl-2 at the G_2/M phase in normal cells as well as in cells exposed to paclitaxel [54]. Phosphorylated Bcl-2 binds with less affinity to Bax and other BH3-only proteins like Bim affecting the control of calcium release and overall apoptotic activity. Thus, this posttranslational modification of Bcl-2 affecting its binding to Bax may alter a critical ratio of these proteins that play pivotal roles in apoptosis [55,56]. Our data suggest that noscapine may be capable of tipping the balance in favor of cell death through a combination of effects on mitochondria and survival signaling pathways. The fact that noscapine has been shown to cross the blood–brain barrier and demonstrate antitumor efficacy in the complete absence of peripheral neuropathy [17], taken together with our in-vitro findings reported here, underscores the potential

importance of noscapine as a novel agent for use in patients with glioblastoma owing to its low toxicity profile and its potent anticancer activity.

Acknowledgements

This work was supported by a National Institute of Health Grant NS057829 (to E.W.N.) and CA100426 (to D.Z.) and a grant from the Long Island League to Abolish Cancer (to E.W.N.).

References

1 Schiff PB, Fant J, Horwitz SB. Promotion of microtubule assembly in vitro by taxol. *Nature* 1979; **277**:665–667.
2 Abal M, Andreu JM, Barasoain I. Taxanes: microtubule and centrosome targets, and cell cycle dependent mechanisms of action. *Curr Cancer Drug Targets* 2003; **3**:193–203.
3 Bhalla KN. Microtubule-targeted anticancer agents and apoptosis. *Oncogene* 2003; **22**:9075–9086.
4 Mollinedo F, Gajate C. Microtubules, microtubule-interfering agents and apoptosis. *Apoptosis* 2003; **8**:413–450.
5 Jordan MA, Wilson L. Microtubules as a target for anticancer drugs. *Nat Rev Cancer* 2004; **4**:253–265.
6 Attard G, Greystoke A, Kaye S, De Bono J. Update on tubulin-binding agents. *Pathol Biol (Paris)* 2006; **54**:72–84.
7 Newcomb EW, Lukyanov Y, Schnee T, Ali MA, Lan L, Zagzag D. Noscapine inhibits hypoxia-mediated HIF-1α expression and angiogenesis in vitro: a novel function for an old drug. *Int J Oncol* 2006; **28**:1121–1130.
8 Ye K, Ke Y, Keshava N, Shanks J, Kapp JA, Tekmal RR, *et al*. Opium alkaloid noscapine is an antitumor agent that arrests metaphase and induces apoptosis in dividing cells. *Proc Natl Acad Sci U S A* 1998; **95**:1601–1606.
9 Mahmoudian M, Mehrpour M, Benaissa F, Siadatpour Z. A preliminary report on the application of noscapine in the treatment of stroke. *Eur J Clin Pharmacol* 2003; **59**:579–581.
10 Zhou J, Panda D, Landen JW, Wilson L, Joshi HC. Minor alteration of microtubule dynamics causes loss of tension across kinetochore pairs and activates the spindle checkpoint. *J Biol Chem* 2002; **277**: 17200–17208.
11 Mooraki A, Jenabi A, Jabbari M, Zolfaghari MI, Javanmardi SZ, Mahmoudian M, *et al*. Noscapine suppresses angiotensin converting enzyme inhibitors-induced cough. *Nephrology (Carlton)* 2005; **10**:348–350.
12 Mahmoudian M, Mojaverian N. Effect of noscapine, the antitussive opioid alkaloid, on bradykinin-induced smooth muscle contraction in the isolated ileum of the guinea-pig. *Acta Physiol Hung* 2001; **88**:231–237.
13 Aneja R, Vangapandu SN, Lopus M, Chandra R, Panda D, Joshi HC. Development of a novel nitro-derivative of noscapine for the potential treatment of drug-resistant ovarian cancer and T-cell lymphoma. *Mol Pharmacol* 2006; **69**:1801–1809.
14 Heidari N, Goliaei B, Moghaddam PR, Rahbar-Roshandel N, Mahmoudian M. Apoptotic pathway induced by noscapine in human myelogenous leukemic cells. *Anticancer Drugs* 2007; **18**:1139–1147.
15 Ke Y, Ye K, Grossniklaus HE, Archer DR, Joshi HC, Kapp JA. Noscapine inhibits tumor growth with little toxicity to normal tissues or inhibition of immune responses. *Cancer Immunol Immunother* 2000; **49**:217–225.
16 Landen JW, Lang R, McMahon SJ, Rusan NM, Yvon AM, Adams AW, *et al*. Noscapine alters microtubule dynamics in living cells and inhibits the progression of melanoma. *Cancer Res* 2002; **62**:4109–4114.
17 Landen JW, Hau V, Wang M, Davis T, Ciliax B, Wainer BH, *et al*. Noscapine crosses the blood-brain barrier and inhibits glioblastoma growth. *Clin Cancer Res* 2004; **10**:5187–5201.
18 Aneja R, Zhou J, Vangapandu SN, Zhou B, Chandra R, Joshi HC. Drug-resistant T-lymphoid tumors undergo apoptosis selectively in response to an antimicrotubule agent, EMO11. *Blood* 2006; **107**: 2486–2492.
19 Aneja R, Lopus M, Zhou J, Vangapandu SN, Ghaleb A, Yao J, *et al*. Rationale design of the microtubule-targeting anti-breast cancer drug EM015. *Cancer Res* 2006; **66**:3782–3791.
20 Tulpule A, Levine AM, Berman NE, Smith L, Auerbach A, Douer D. Phase I study of noscapine for patients with non-Hodgkin's lymphoma or chronic lymphocytic leukemia refractory to chemotherapy. *Blood* 2005; **106**:3341.
21 Alonso M, Tamasdan C, Miller DC, Newcomb EW. Flavopiridol induces apoptosis in glioma cell lines independent of retinoblastoma and p53 tumor suppressor pathway alterations by a caspase-independent pathway. *Mol Cancer Ther* 2003; **2**:139–150.
22 Zagzag D, Nomura M, Friedlander DR, Blanco CY, Gagner JP, Nomura N, *et al*. Geldanamycin inhibits migration of glioma cells in vitro: a potential role for hypoxia-inducible factor (HIF-1α) in glioma cell invasion. *J Cell Physiol* 2003; **196**:394–402.
23 Nomura M, Nomura N, Newcomb EW, Lukyanov Y, Tamasdan C, Zagzag D. Geldanamycin induces mitotic catastrophe and subsequent apoptosis in human glioma cells. *J Cell Physiol* 2004; **201**:374–384.
24 Newcomb EW, Ali MA, Schnee T, Lan L, Lukyanov Y, Fowkes M, *et al*. Flavopiridol downregulates hypoxia-mediated hypoxia-inducible factor-1α expression in human glioma cells by a proteasome-independent pathway: implications for in vivo therapy. *Neuro-oncol* 2005; **7**:225–235.
25 Newcomb EW, Lymberis SC, Lukyanov Y, Shao Y, Schnee T, Devitt ML, *et al*. Radiation sensitivity of GL261 murine glioma model and enhanced radiation response by flavopiridol. *Cell Cycle* 2006; **5**:93–99.
26 Newcomb EW, Lukyanov Y, Schnee T, Esencay M, Fischer I, Hong D, *et al*. The geldanamycin analogue 17-allylamino-17-demethoxygeldanamycin inhibits the growth of GL261 glioma cells in vitro and in vivo. *Anticancer Drugs* 2007; **18**:875–882.
27 Ishii N, Maier D, Merlo A, Tada M, Sawamura Y, Diserens AC, *et al*. Frequent co-alterations of TP53, p16/CDKN2A, $p14^{ARF}$, PTEN tumor suppressor genes in human glioma cell lines. *Brain Pathol* 1999; **9**:469–479.
28 Leverrier S, Bergamaschi D, Ghali L, Ola A, Warnes G, Akgul B, *et al*. Role of HPV E6 proteins in preventing UVB-induced release of pro-apoptotic factors from the mitochondria. *Apoptosis* 2007; **12**:549–560.
29 Davis FM, Tsao TY, Fowler SK, Rao PN. Monoclonal antibodies to mitotic cells. *Proc Natl Acad Sci U S A* 1983; **80**:2926–2930.
30 Muehlbauer PA, Schuler MJ. Measuring the mitotic index in chemically-treated human lymphocyte cultures by flow cytometry. *Mutat Res* 2003; **537**:117–130.
31 Haldar S, Chintapalli J, Croce CM. Taxol induces bcl-2 phosphorylation and death of prostate cancer cells. *Cancer Res* 1996; **56**:1253–1255.
32 Blagosklonny MV, Bishop PC, Robey R, Fojo T, Bates SE. Loss of cell cycle control allows selective microtubule-active drug-induced Bcl-2 phosphorylation and cytotoxicity in autonomous cancer cells. *Cancer Res* 2000; **60**:3425–3428.
33 Ling Y-H, Jiang J-D, Holland JF, Perez-Soler R. Arsenic trioxide produces polymerization of microtubules and mitotic arrest before apoptosis in human tumor cell lines. *Mol Pharmacol* 2002; **62**:529–538.
34 Kolfschoten GM, Hulscher TM, Duyndam MCA, Pinedo HM, Boven E. Variation in the kinetics of caspase-3 activation, Bcl-2 phosphorylation and apoptotic morphology in unselected human ovarian cancer cell lines as a response to docetaxel. *Biochem Pharmacol* 2002; **63**:733–743.
35 Borgne A, Meijer L. Sequential desphosphorylation of p34(cdc2) on Thr-14 and Tyr-15 at the prophase/metaphase transition. *J Biol Chem* 1996; **271**:27847–27854.
36 Fortugno P, Wall NR, Giodini A, O'Connor DS, Plescia J, Padgett KM, *et al*. Survivin exists in immunochemically distinct subcellular pools and is involved in spindle microtubule function. *J Cell Sci* 2002; **115**:575–585.
37 Zhou J, Gupta K, Yao J, Ye K, Panda D, Giannakakou P, *et al*. Paclitaxel-resistant human ovarian cancer cells undergo c-Jun NH_2-terminal kinase-mediated apoptosis in response to noscapine. *J Biol Chem* 2002; **43**:39777–39785.
38 Wang TH, Popp DM, Wang HS, Saitoh M, Mural JG, Henley DC, *et al*. Microtubule dysfunction induced by paclitaxel initiates apoptosis through both c-Jun N-terminal kinase (JNK)-dependent and -independent pathways in ovarian cancer cells. *J Biol Chem* 1999; **274**:8208–8216.
39 Weiderhold KN, Randall-Hlubek DA, Polin LA, Hamel E, Mooberry SL. CB694, a novel antimitotic with antitumor activities. *Int J Cancer* 2006; **118**:1032–1040.
40 Shtil AA, Mandlekar S, Yu R, Walter RJ, Hagen K, Tan TH, *et al*. Differential regulation of mitogen-activated protein kinases by microtubule-binding agents in human breast cancer cells. *Oncogene* 1999; **18**:377–384.
41 Stone AA, Chambers TC. Microtubule inhibitors elicit differential effects on MAP kinase (JNK, ERK, and p38) signaling pathways in human KB-3 carcinoma cells. *Exp Cell Res* 2000; **254**:110–119.
42 Tinley TL, Randall-Hlubek DA, Leal RM, Jackson EM, Cessac JW, Quade JC Jr, *et al*. Taccalonlides E and A: plant-derived steroids with microtubule-stabilizing activity. *Cancer Res* 2003; **63**:3211–3220.
43 Aneja R, Ghaleb AM, Zhou J, Yang VW, Joshi HC. p53 and p21 determine the sensitivity of noscapine-induced apoptosis in colon cancer cells. *Cancer Res* 2007; **67**:3862–3870.

44 Castedo M, Perfettini J-L, Roumier T, Andreau K, Medema R, Kroemer G. Cell death by mitotic catastrophe: a molecular definition. *Oncogene* 2004; **23**:2825–2837.

45 Galluzzi L, Maiuri MC, Vitale I, Zischka H, Castedo M, Zitvogel L, *et al.* Cell death modalities: classification and pathophysiological implications. *Cell Death Differ* 2007; **14**:1237–1266.

46 Aneja R, Dhiman N, Idnani J, Awasthe A, Arora SK, Chandra R, *et al.* Preclinical pharmacokinetics and bioavailability of noscapine, a tubulin-binding anticancer agent. *Cancer Chemother Pharmacol* 2007; **60**: 831–839.

47 Xia Z, Dickens M, Raingeaud J, Davis RJ, Greenberg ME. Opposing effects of ERK and JNK-p38 MAP kinases on apoptosis. *Science* 1995; **270**:1326–1331.

48 Ambrose M, Ryan A, O'Sullivan GC, Dunne C, Barry OP. Induction of apoptosis in renal cell carcinoma by reactive oxygen species: involvement of extracellular signal-regulated kinase 1/2, p38δ/γ, cycloooxygenase-2 down-regulation, and translocation of apoptosis-inducing factor. *Mol Pharmacol* 2006; **69**:1879–1890.

49 Seidman R, Gitelman I, Sagi O, Horwitz SB, Wolfson M. The role of ERK 1/2 and p38MAP-kinase pathways in taxol-induced apoptosis in human ovarian carcinoma cells. *Exp Cell Res* 2001; **268**:84–92.

50 Mansilla S, Priebe W, Portugal J. Mitotic catastrophe results in cell death by caspase-dependent and caspase-independent mechanisms. *Cell Cycle* 2006; **5**:53–60.

51 Gao N, Rahmani M, Dent P, Grant S. 2-methoxyestradiol-induced apoptosis in human leukemia cells proceeds through a reactive oxygen species and Akt-dependent process. *Oncogene* 2005; **24**:3793–3809.

52 Yacoub A, Park MA, Hanna D, Hong Y, Mitchell C, Pandya AP, *et al.* OSU-03012 promotes caspase-independent but PERK-, cathepsin B-, BID, and AIF-dependent killing of transformed cells. *Mol Pharmaol* 2006; **70**:589–603.

53 Srivastava RK, Mi Q-S, Hardwick JM, Longo DL. Deletion of the loop region of Bcl-2 completely blocks paclitaxel-induced apoptosis. *Proc Natl Acad Sci U S A* 1999; **96**:3775–3780.

54 Yamamoto K, Ichijo H, Korsmeyer SJ. BCL-2 is phosphorylated and inactivated by an ASK1/Jun N-terminal protein kinase pathway normally activated at G(2)M. *Mol Cell Biol* 1999; **19**:8469–8478.

55 Korsmeyer SJ, Shutter JR, Veis DJ, Merry DE, Oltvai ZN. Bcl-2/Bax: a rheostat that regulates an anti-oxidant pathway and cell death. *Semin Cancer Biol* 1993; **4**:327–332.

56 Kroemer G, Reed JC. Mitochondrial control of cell death. *Nat Med* 2000; **6**:513–519.